

Nonlinear photon transport in a semiconductor waveguide-cavity system containing a single quantum dot: Anharmonic cavity-QED regime

S. Hughes* and C. Roy

Department of Physics, Queen's University, Kingston, Ontario, Canada K7L 3N6

(Received 4 August 2011; revised manuscript received 19 December 2011; published 17 January 2012)

We present a semiconductor master equation technique to study the input/output characteristics of coherent photon transport in a semiconductor waveguide-cavity system containing a single quantum dot. We use this approach to investigate the effects of photon propagation and anharmonic cavity-QED for various dot-cavity interaction strengths, including weakly-coupled, intermediately-coupled, and strongly-coupled regimes. We demonstrate that for mean photon numbers much less than 0.1, the commonly adopted weak excitation (single quantum) approximation breaks down, even in the weak coupling regime. As a measure of the multiphoton correlations, we compute the Fano factor and the correlation error associated with making a semiclassical approximation. We also explore the role of electron-acoustic-phonon scattering and find that phonon-mediated scattering plays a qualitatively important role on the light propagation characteristics. As an application of the theory, we simulate a conditional phase gate at a phonon bath temperature of 20 K in the strong coupling regime.

DOI: [10.1103/PhysRevB.85.035315](https://doi.org/10.1103/PhysRevB.85.035315)

PACS number(s): 42.50.Ct, 42.50.Pq, 78.67.Hc

I. INTRODUCTION

The ability to couple waveguides and cavities offers exciting opportunities for integrated quantum optical devices using solids.^{1–3} In particular, planar photonic crystals offer a technology platform, where quantum bits (qubits) can be manipulated from quantum dots (QDs) placed at field antinode positions within the cavity or waveguide.^{4–6} Integrated semiconductor micropillar systems also show great promise for quantum optical applications,^{7,8} working at the few photon level.

Recently, there have been several successful demonstrations of coherent light propagation effects in various semiconductor systems, including planar photonic crystals and micropillars. Bose *et al.*⁹ measured the exciton-induced doublet (polariton splitting) through waveguide mode transmission in a photonic crystal waveguide-cavity system¹⁰ [cf. Fig. 1(a)], while Loo *et al.*¹¹ probed the strong coupling in a micropillar via coherent reflection [cf. Fig. 1(b)]; Young *et al.*¹² demonstrated first steps toward a conditional phase gate using light reflection from a micropillar. Common to the analysis of all of these experiments has been the application of the *weak excitation approximation* (WEA), where at most only one quantum is assumed. For example, Ref. 12 suggested that their experiments were likely at the “single photon level” for less than 0.1 photons per cavity lifetime, so they applied a WEA solution. The same assumptions are tacitly made by many other groups, in excitation regimes where the mean photon number is well below those associated with saturating the QD exciton.¹³ These useful formalisms have been very successful and certainly help to clarify the basic physics of low-intensity photon transport.

For increasing field strengths, however, the validity for the WEA becomes questionable, and there can be quantum nonlinearities in the system due to multiphoton correlations. Giant optical nonlinearities were studied by Auffèves-Garnier *et al.*,¹⁴ their semiclassical approach adiabatically eliminated the cavity mode and included effects outside the WEA (the “Purcell regime”); naturally with such a semiclassical approach, there is no influence from the higher lying levels of

the *anharmonic* Jaynes-Cumming (JC) ladder, so it cannot be applied in the strong-coupling regime. Most photon transport approaches also neglect the details of electron-acoustic phonon scattering^{15–19}—apart from the inclusion of a Lorentzian decay rate for the exciton, i.e., broadening of the zero phonon line (ZPL). Recently, several works have shown that coherent excitation of semiconductor-QD systems can easily go into the anharmonic cavity-QED (quantum electrodynamics) regime.^{20,21} Thus the questions arise: (i) To what extent can one safely employ the WEA for these emerging semiconductor waveguide-cavity and micropillar systems? (ii) When are multiphoton correlation effects important (quantum nonlinear regime)? (iii) What is the role of electron-acoustic phonon scattering and how does this mechanism differ from a simple-Lorentzian pure dephasing model?

In this work we attempt to answer these questions for the regime of coherent photon transport, and show that generally one must include multiphoton effects and phonon scattering within the theoretical formalism. Even in the weak coupling regime, higher-order quantum correlation effects are shown to be significant. Our paper is organized as follows: In Sec. II, we introduce the general theoretical technique to simulate coherent photon transport outside both the WEA and the semiclassical approximation. The theory is based on a quantum master-equation (ME) formalism where cavity and dot decays are introduced by Lindblad superoperators, and phonon interactions are included from an effective phonon ME²² that includes electron-phonon interactions at a microscopic level—derived using a polaron transform.^{20,22} In Sec. III, we first present calculations with no acoustic phonon coupling, for several different QD-cavity couplings; both the weak-coupling regime and the intermediate-to-strong coupling regime are investigated. We demonstrate that substantial deviations from the WEA can result, even for very small mean photon numbers $\ll 0.1$. We then modify the ME approach to include the mechanism of electron-acoustic-phonon scattering, and study the impact of electron-phonon interactions on incoherent scattering and on coherent renormalization of the exciton-cavity coupling rate; qualitative differences from a simple Lorentzian

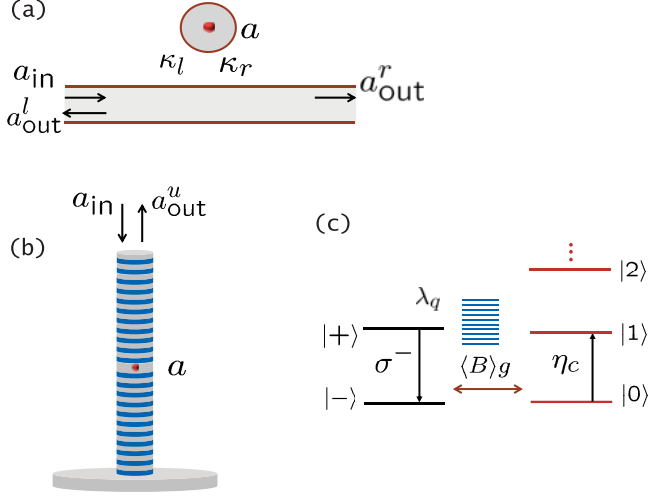


FIG. 1. (Color online) Schematic of two semiconductor cavity-QED systems containing a quantum dot: (a) waveguide-cavity system (e.g., made up of a planar photonic crystal) where we assume $\kappa_l = \kappa_r = 2\kappa_0$ (where κ_0 is the out of plane loss), and (b) a micropillar cavity. (c) Dot and cavity energy levels, where the exciton system ($|+\rangle/|-\rangle$) interacts with an acoustic phonon bath (see text).

decay model are found. As an application of the theory, we study the transmission of light in the strong-coupling regime and simulate a conditional (exciton-induced) phase gate. We conclude in Sec. IV.

II. THEORY

We wish to describe light propagation for a QD-cavity geometry, where the input and output fields can be identified separately from the cavity region in which the QD is assumed to be embedded. An example waveguide-cavity system is shown schematically in Fig. 1(a). For a continuous wave (cw) waveguide mode of a photonic crystal system, the classical WEA reflectivity was previously derived by Hughes and Kamada:^{10,23}

$$r_{pc}(\omega) = \frac{i\omega\Gamma_c}{\omega_c^2 - \omega^2 - i\omega(\Gamma_c + \Gamma_0) - \omega\Sigma(\omega)}, \quad (1)$$

where the self-energy $\omega\Sigma(\omega) = \omega g^2/(\omega_x - \omega - i\omega\Gamma_x^t)$, $\Gamma_0 \equiv 2\kappa_0$ is the cavity decay rate through vertical scattering (unloaded cavity broadening), $\Gamma_c \equiv 2\kappa_c = 2(\kappa_l + \kappa_r)$ is the cavity-waveguide coupling rate (which is inversely proportional to the group velocity of the waveguide mode¹⁰), ω_c is the cavity mode resonance, ω_x is the target exciton resonance of the QD, and $\Gamma_x^t = \gamma + \gamma'$ is the total decay rate of the exciton—including radiative (γ) and nonradiative, pure dephasing (γ') processes. The total cavity decay rate is $\Gamma_c^t = \Gamma_0 + \Gamma_c$ and the exciton-cavity coupling rate, $g \propto d^2/V_{\text{eff}}$, where d is the dipole moment of the exciton and V_{eff} is the effective mode volume. The corresponding transmissivity is simply $t = 1 + r$, and one can also define the reflection and transmission, through $R = |r|^2$ and $T = |t|^2$. Similar expressions have been derived by other groups, e.g., Refs. 14, 24, and 25. With the dot on resonance with the cavity, then a polariton doublet coincides with the vacuum Rabi splitting which can be observed in transmission or reflection;

this *normal mode* doublet can occur even if the dot is *not* in the strong-coupling regime,^{14,24,26} though ultimately the doublet feature is lost at high temperatures due to phonon bath coupling.¹⁶ The analysis of coherent reflection from a micropillar system is similar; one has $r_{\text{micropillar}} = 1 - \sqrt{\eta} r_{pc}$, where η is a measure of in/out coupling efficiency,¹¹ and one also makes the following replacements: $\Gamma_c \rightarrow \Gamma_0$ (vertical scattering) and $\Gamma_0 \rightarrow \Gamma_s$ (sidewall scatter).

The above WEA formalism does not distinguish between radiative and pure dephasing processes of the QD exciton (which a semiclassical approach can); nor does it take into consideration the acoustic phonon bath or multiphoton effects. Ignoring the complexities of phonon scattering for now^{16,18,19}—which we will introduce below—these analytical formulas are expected to work for only weak excitation conditions (strictly linear), and for pure dephasing rates,⁹ $\gamma' \ll g^2\Gamma_c^t/[4(\omega_c - \omega)^2 + (\Gamma_c^t/2)^2]$.

To go beyond the WEA, and the semiclassical approaches, we will use a ME approach where exciton-phonon interactions are easily included to all orders. Referring to Fig. 1(a), we relate the left/right output operators to the cavity mode operator through²⁷

$$\langle a_{\text{out}}^r(t) \rangle = -\langle a_{\text{in}}(t) \rangle + \sqrt{2\kappa_c} \langle a(t) \rangle, \quad (2)$$

$$\langle a_{\text{out}}^l(t) \rangle = \sqrt{2\kappa_c} \langle a(t) \rangle, \quad (3)$$

where, for a coherent cw input state, $\langle a_{\text{in}} \rangle = i\eta_c/(2\sqrt{2\kappa_c})$, with η_c the cavity pump rate. Following the solution of the ME (discussed below), the *steady-state* transmissivity and reflectivity are obtained: $t \equiv |t|e^{i\phi_t} = \langle a_{\text{out}}^r \rangle_{ss}/\langle a_{\text{in}} \rangle$ and $r \equiv |r|e^{i\phi_r} = \langle a_{\text{out}}^l \rangle_{ss}/\langle a_{\text{in}} \rangle$, where ϕ_t and ϕ_r are the phases. Working in a frame rotating with respect to the laser pump frequency, ω_L , the model Hamiltonian can be written as

$$H = \hbar\Delta_{xL}\sigma^+\sigma^- + \hbar\Delta_{cL}a^\dagger a + \hbar g(\sigma^+ a + a^\dagger \sigma^-) + H_{\text{drive}}^c + \sigma^+\sigma^- \sum_q \hbar\lambda_q(b_q + b_q^\dagger) + \sum_q \hbar\omega_q b_q^\dagger b_q, \quad (4)$$

where b_q (b_q^\dagger) are the annihilation and creation operators of the phonons, a is the cavity mode annihilation operator, σ^+ and σ^- are Pauli operators of the electron-hole pair (exciton), $\Delta_{\alpha L} \equiv \omega_\alpha - \omega_L$ ($\alpha = x, c$) are the detunings of the exciton (ω_x) and cavity (ω_c) from ω_L , and $H_{\text{drive}}^c = \hbar\eta_c(a + a^\dagger)$ describes the *coherent* cavity drive (excited through the waveguide channel).

To obtain the ME, we first transform Eq. (4) to a polaron frame, which formally recovers the independent boson model (IBM);^{28–30} the IBM is known to accurately describe the characteristic line shape of a single exciton coupled to a bath of acoustic phonons.¹⁵ Specifically, the polaron ME^{20,30,31} introduces coherent electron-phonon coupling exactly, while incoherent phonon interactions are treated at the level of a second-order Born approximation. Further details of the model are discussed in Refs. 31 and 20. The time-convolutionless ME takes the form^{20,31}

$$\frac{\partial \rho}{\partial t} = \frac{1}{i\hbar} [H'_{\text{sys}}, \rho(t)] + \mathcal{L}(\rho) + \mathcal{L}_{\text{ph}}(\rho), \quad (5)$$

where the polaron-transformed system Hamiltonian is $H'_{\text{sys}} = \hbar(\Delta_{xL} - \Delta_P)\sigma^+\sigma^- + \hbar\Delta_{cL}a^\dagger a + \langle B \rangle X_g + H'_{\text{drive}}$, with $\langle B \rangle = \exp[-\frac{1}{2} \int_0^\infty d\omega J(\omega)/\omega^2 \coth(\beta\hbar\omega/2)]$ ($\beta = 1/k_B T$), $X_g = \hbar g(a^\dagger\sigma^- + \sigma^+a)$, and $\Delta_P = \int_0^\infty d\omega J(\omega)/\omega$. In what follows, we will absorb the polaron shift (Δ_P) into the definition of ω_x . The phonon spectral function,^{20,31,32} $J(\omega) = \alpha_p \omega^3 \exp(-\omega^2/2\omega_b^2)$, describes electron-acoustic phonon interaction via a deformation potential coupling.

Using a Markov approximation, the incoherent phonon scattering term is defined as²⁰

$$\mathcal{L}_{\text{ph}}(\rho) = -\frac{1}{\hbar^2} \int_0^\infty d\tau \sum_{m=g,u} (G_m(\tau) \times [X_m, e^{-iH'_{\text{sys}}\tau/\hbar} X_m e^{iH'_{\text{sys}}\tau/\hbar} \rho(t)] + \text{H.c.}), \quad (6)$$

where $X_u = -i\hbar g(a^\dagger\sigma^- - \sigma^+a)$, and $G_{g/u}(t)$ are the polaron Green functions:^{28,30} $G_g(t) = \langle B \rangle^2 (\cosh[\phi(t)] - 1)$, $G_u(t) = \langle B \rangle^2 \sinh[\phi(t)]$, with $\phi(t) = \int_0^\infty d\omega \frac{J(\omega)}{\omega^2} [\coth(\beta\hbar\omega/2) \cos(\omega t) - i \sin(\omega t)]$. In Ref. 22, an effective Lindblad ME has been shown to yield very good agreement with the full polaron ME solution above. In this way, one defines the phonon-mediated incoherent scattering processes through

$$\mathcal{L}_{\text{ph}}(\rho) = \frac{\Gamma_{\text{ph}}^{\sigma^+a}}{2} \mathcal{L}(\sigma^+a) + \frac{\Gamma_{\text{ph}}^{a^\dagger\sigma^-}}{2} \mathcal{L}(a^\dagger\sigma^-), \quad (7)$$

where $\mathcal{L}(D) = 2D\rho D^\dagger - D^\dagger D\rho - \rho D^\dagger D$, and the scattering rates are obtained analytically, from²²

$$\Gamma_{\text{ph}}^{\sigma^+a/a^\dagger\sigma^-} = 2 \langle B \rangle^2 g^2 \text{Re} \left[\int_0^\infty d\tau e^{\pm i\Delta_{cx}\tau} (e^{\phi(\tau)} - 1) \right], \quad (8)$$

where $\Delta_{cx} = \omega_c - \omega_x$ is the cavity-exciton detuning. The rate $\Gamma_{\text{ph}}^{a^\dagger\sigma^-}$ describes the process of cavity excitation and the emission of an exciton, via phonon-induced scattering, and $\Gamma_{\text{ph}}^{\sigma^+a}$ describes exciton excitation via the emission of a cavity photon. For completeness, one can also add in the Stark shifts,²⁰ but these are found to be negligible for the regimes considered in this work. Since this Lindblad-ME form is considerably easier to work with and helps to identify the physics of the scattering processes in a more transparent way, we will use this latter form for our phonon calculations in this paper. An alternative weak-phonon-coupling theory is presented in Ref. 33.

Phenomenologically, we also include Liouvillian superoperators:^{20,32}

$$\begin{aligned} \mathcal{L}(\rho) = & \frac{\tilde{\gamma}}{2} (2\sigma^- \rho \sigma^+ - \sigma^+ \sigma^- \rho - \rho \sigma^+ \sigma^-) \\ & + \kappa_i (2a\rho a^\dagger - a^\dagger a \rho - \rho a^\dagger a) \\ & + \frac{\gamma'}{2} (\sigma_{11} \rho \sigma_{11} - \sigma_{11} \sigma_{11} \rho - \rho \sigma_{11} \sigma_{11}), \end{aligned} \quad (9)$$

where $2\kappa_i = 2\kappa_0 + 2\kappa_w \equiv \Gamma'_c$, $\tilde{\gamma} = \gamma \langle B \rangle^2$ is the radiative decay rate of the exciton, γ' is the pure dephasing rate of the exciton, and $\sigma_{11} = \sigma^+\sigma^-$. Figure 1(c) shows a schematic of the model, which we solve in a basis of $|n\rangle$ photons and the two QD states $|-\rangle/|+\rangle$. The WEA corresponds to a three-state model, i.e., only including the ground state and the first two ladder states of the JC model.

For suitably large input fields, many JC ladder states may be involved. To better highlight the role of quantum statistics in the system and to help quantify the possible failure of a semiclassical approximation, we introduce a function for computing the relative *correlation error* (CE) in the expectation $\langle a^\dagger\sigma^- \rangle_{\text{ss}}$ compared to $\langle a^\dagger \rangle_{\text{ss}} \langle \sigma^- \rangle_{\text{ss}}$,

$$\text{CE} = \frac{|\langle a^\dagger\sigma^- \rangle_{\text{ss}} - \langle a^\dagger \rangle_{\text{ss}} \langle \sigma^- \rangle_{\text{ss}}|}{|\langle a^\dagger\sigma^- \rangle_{\text{ss}}|}, \quad (10)$$

where 100 CE is the percentage relative error; in a semiclassical picture, of course CE = 0. We also compute the mean photon variance, defined through the Fano factor:

$$F = \frac{\langle (a^\dagger a)^2 \rangle_{\text{ss}} - \langle a^\dagger a \rangle_{\text{ss}}^2}{\langle a^\dagger a \rangle_{\text{ss}}}. \quad (11)$$

III. RESULTS

A. Photon transport with no acoustic phonon coupling

We first investigate the system with no acoustic phonon coupling—apart from the ZPL broadening (i.e., no \mathcal{L}_{ph} process and $\langle B \rangle = 1$). For calculations, we use material parameters that correspond closely to those in experiments: $\tilde{\gamma} = 1 \mu\text{eV}$, $\kappa_c = 4\kappa_0 = 50 \mu\text{eV}$, $\gamma' = 4 \mu\text{eV}$ (unless stated otherwise), and we will study various values of g and η_c .

In Fig. 2 we study the weak-coupling regime, with $g = 20 \mu\text{eV} \approx 0.32\kappa_i$, using a fairly weak excitation field of

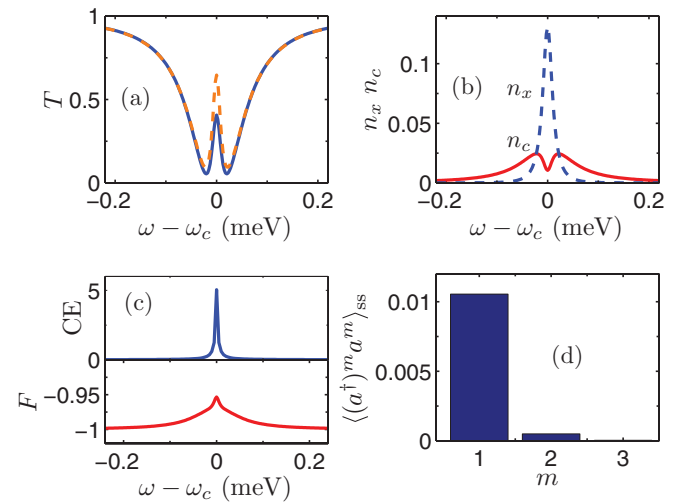


FIG. 2. (Color online) Transmission characteristics for a weakly-coupled QD-cavity-waveguide system, with $g = 20 \mu\text{eV} \approx 0.32 \kappa_i$ and $\eta_c = 0.5g$. (a) Transmission with (dashed) and without (solid) the WEA approximation. All other calculations in (b)–(d) use the full multiphoton approach. (b) Steady-state cavity (solid) and exciton (cavity) populations. (c) Relative correlation error of $\langle a^\dagger\sigma^- \rangle_{\text{ss}}$ if a semiclassical approximation was used, CE, and the Fano factor (photon number variance). (d) Cavity photon moments $\langle (a^\dagger)^m a^m \rangle_{\text{ss}}$ versus m . The other parameters are as follows: $\tilde{\gamma} = 1 \mu\text{eV}$, $\gamma' = 4 \mu\text{eV}$, and $\kappa_c = 50 \mu\text{eV}$ ($\kappa_i = 62.5 \mu\text{eV}$). Of note, the polariton doublet in (a) is not due to strong coupling, since we are in the weak coupling regime for these simulations (see text).

$\eta_x = 0.5g$. This field value was chosen to be small enough that the cavity population is significantly lower than 0.1, but large enough to see a breakdown of the WEA. We have also confirmed that this value of g/κ yields no vacuum Rabi splitting. In Fig. 2(a) we show the transmission versus detuning with (dashed) and without the WEA (solid); a few comments are in order: (i) we confirm that the polariton doublet appears even though we are not in the strong-coupling regime (also see Refs. 14, 24, and 26); (ii) the WEA breaks down with already qualitative differences of more than 40% near $\omega \approx \omega_c$; and (iii) with the chosen value of g , the region of “transparency” is notably very weak, which is a consequence of the finite QD broadening (through $\tilde{\gamma}$ and γ'). This latter observation can be contrasted with the results in Ref. 14 where such broadenings were not included; these ZPL broadenings are essential to include for a realistic QD system. In Fig. 2(b), we show the (numerically exact) exciton and cavity-mode populations, confirming that the largest cavity population is well below 0.1; we note that the fundamental condition for the WEA is not a low number of photons, but a negligible excitation of the dot—and the exciton population is evidently no longer negligible. In Fig. 2(c), we display the correlation error, CE, and the Fano factor, F . Even at these weak drives and small g (weak-coupling regime), it is clear that a semiclassical approximation can fail, especially near $\omega \approx \omega_c$, where the percentage error of assuming $\langle a^\dagger \sigma^- \rangle_{ss} \approx \langle a^\dagger \rangle_{ss} \langle \sigma^- \rangle_{ss}$ is as much as 50%. In Fig. 2(d), we plot the corresponding cavity-photon moments $\langle (a^\dagger)^m a^m \rangle_{ss}$ for the first few photon states, which suggest that only the first two photon number states are excited.

To better probe the nonlinear quantum aspects of this dot-cavity coupling regime, in Fig. 3 we increase the pump value to $\eta_c = 2.5g$. Here the WEA breaks down dramatically, as shown by Fig. 3(a); Figs. 3(c) and 3(d) further confirm that we are accessing a regime where both the WEA and the semiclassical approximations may fail, even for a weakly coupled system. We are thus already in the anharmonic cavity-QED regime. Figure 3(b) shows the corresponding populations.

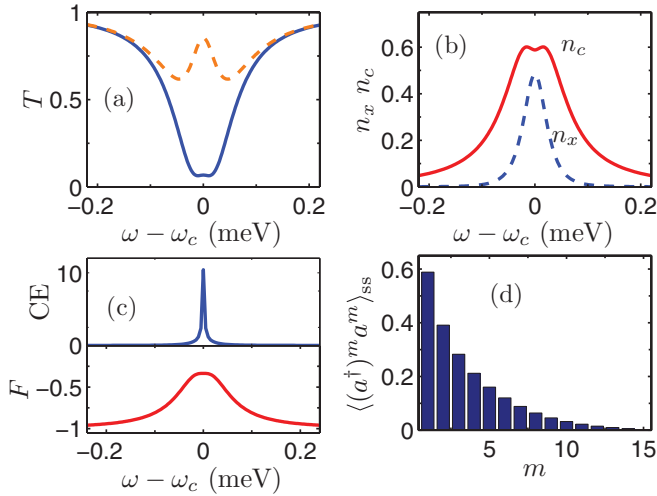


FIG. 3. (Color online) As in Fig. 2, but with the larger pump field $\eta_c = 2.5g$. We clearly see that multiphoton correlations are needed, even for this weakly coupled system ($g \ll \kappa_t$).

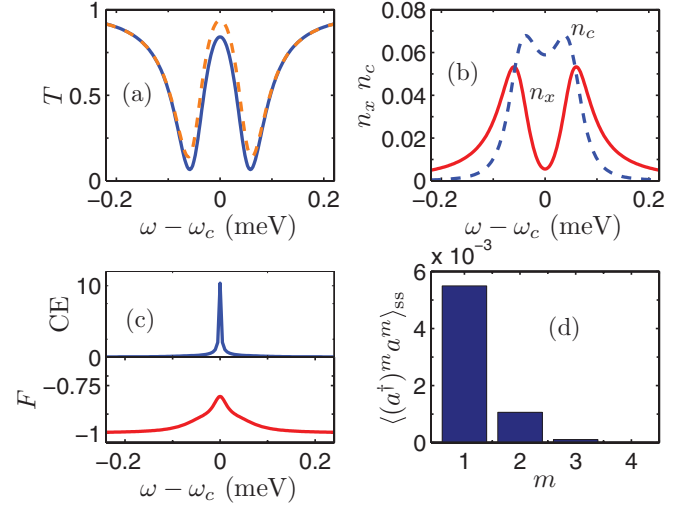


FIG. 4. (Color online) As in Fig. 2, but for an intermediate-to-strongly coupled system, with $g = 60 \mu\text{eV} \approx \kappa_t$, and $\eta_c = 0.25g$. The other parameters are the same as in Fig. 2.

Next, we investigate a QD-cavity system in the weak-to-intermediate coupling regime, with $g = 60 \mu\text{eV} \approx \kappa_t$, and $\eta_c = 0.25g$. In Fig. 4(a), we show the transmission with (dashed) and without (solid) the WEA; we also show the populations [Fig. 4(b)], the semiclassical error [Fig. 4(c)], and the Fano factor [Fig. 4(d)]. For this relatively weak drive, we again observe noticeable differences in the WEA and non-WEA predictions; we also recognize that higher-order photon moments are significant already in the $m = 2$ photon state [Fig. 4(d)].

With increasing drives, namely, when $\eta_c = 1.2g$, Fig. 5 confirms that the differences between the WEA and multiphoton calculations are even more dramatic (as expected), and the on-resonance transmission becomes much smaller with the nonlinear drive.¹⁴ Indeed, we recognize that multiphoton

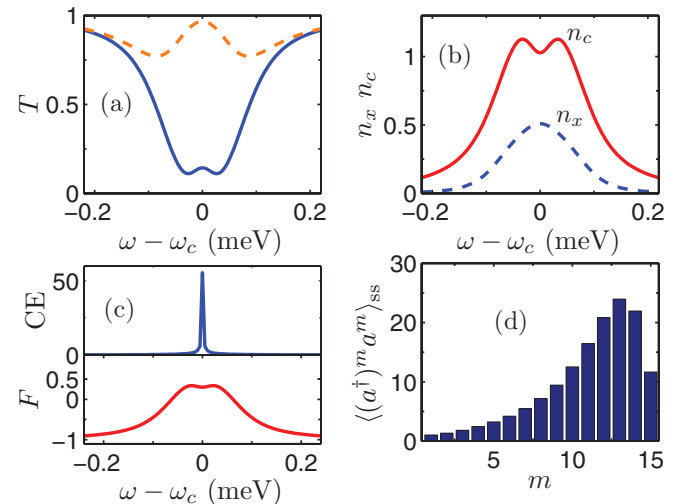


FIG. 5. (Color online) As in Fig. 4, but with the larger pump field $\eta_c = 1.2g$.

effects are now fairly profound, easily exciting the first 15 photon states. This means that we are now accessing the first 30 states of the JC ladder, with modest exciton-cavity coupling rates (i.e., $g \sim \kappa_I$).

B. Influence of acoustic phonon coupling

For the phonon bath calculations, we use material parameters for InAs QDs,^{18,20} with $\omega_b = 1$ meV and $\alpha_p/(2\pi)^2 = 0.06$ ps². The phonon ME model considers a bath at a temperature of $T = 20$ K, resulting in $\langle B \rangle (20 \text{ K}) = 0.73$. We now consider a QD-cavity system in the strong-coupling regime, with $g = 120 \mu\text{eV} \approx 2\kappa_I$, using a low cavity pump rate of $\eta_c = 0.15g$.

From the theory described in Sec. II, electron-phonon scattering is seen to manifest in a coherent renormalization in $g \rightarrow \langle B \rangle g$ as well as mediate incoherent scattering between the exciton and cavity. To better highlight the role of incoherent scattering separately, we first set $\langle B \rangle = 1$ (i.e., we neglect the coherent phonon effects) for the calculations in Figs. 6(a) and 6(b). Figure 6(a) shows the transmission results with (solid) and without (dashed) incoherent phonon scattering. We recognize a clear change in the maximum and minimum

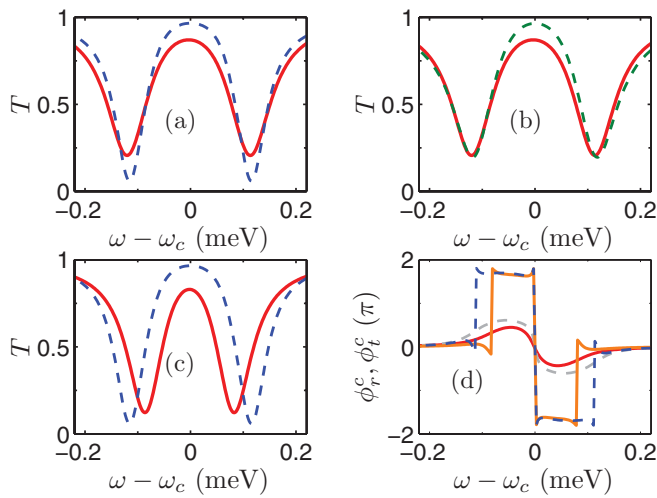


FIG. 6. (Color online) Transmission/reflection characteristics of a weakly excited strongly-coupled system, $\eta_c = 0.15g$, with $g = 120 \mu\text{eV} \approx 2\kappa_I$. The peak exciton and cavity photon populations are both below 0.1 (not shown). For these calculations we also consider the effect of acoustic phonon scattering at a bath temperature of $T = 20$ K. (a) Transmission with (solid) and without (dashed) incoherent photon-scattering terms, included through \mathcal{L}_{ph} ; here we ignore coherent renormalization effects, i.e., $\langle B \rangle = 1$. (b) Transmission as in (a), but now the no-phonon case (dashed) has $\gamma' \rightarrow 1.6\gamma'$ to try and mimic the influence of incoherent phonon scattering. (c) Transmission with (solid) and without (dashed) incoherent scattering and a coherent phonon reduction in $g \rightarrow \langle B \rangle g$ with $\langle B \rangle = 0.73$. (d) Conditional phase gate, where the larger phase changes are ϕ_r^c and the smaller phase change is ϕ_t^c ; solid and dashed lines show results with and without phonon coupling, respectively. All other system and material parameters are the same as in Fig. 2, and no WEA is made (the semiclassical approximation breaks down dramatically in this strong-coupling regime).

transmission regions and a qualitative reshaping of the spectral profile. It is common to try and partially mimic the effects of phonon scattering by using an effective γ' to fit the data. To highlight the differences with such a simple Lorentzian coupling approach, in Fig. 6(b) we try to fit the phonon model by increasing $\gamma' \rightarrow 1.6\gamma'$ (dashed), which naturally broadens the ZPL through an increase of the (Lorentzian model) pure dephasing process. However, comparing the dashed and solid curves of Fig. 6(b), we see that the features near the center peak and the edges of the graph are noticeably different; in particular, a broadened ZPL incorrectly widens the Lorentzian tails and misses the reduction of the center transmission peak. In addition, a change in pure dephasing does not obtain the coherent reduction of g ($g \rightarrow 0.73g$ since $\langle B \rangle = 0.73$ at 20 K), which is an important temperature-dependent effect that we include in Fig. 6(c); this marked reduction in the Rabi splitting will increase with temperature, which is important to note especially if trying to fit experimental data that is probed via temperature tuning. For lower bath temperatures, the on-resonance case can also be asymmetric.¹⁶ We further note that because we are exciting through the cavity mode, the effects of the drive on excitation-induced dephasing are significantly suppressed, which is in contrast to driving through the QD exciton.^{20,31,34,35}

Finally, we study a conditional phase gate. We define the conditional phase through $\phi_{t/r}^c = \phi_{t/r}^d - \phi_{t/r}^0$, where $\phi_{t/r}^d$ includes the dot resonance and $\phi_{t/r}^0$ is the phase without the dot. Using a semiconductor micropillar system, conditional phase shifts of around 0.03 rad were recently observed.¹² Figure 6(d) shows the conditional phases, with (solid) and without (dashed) phonon coupling. Near the spectral regions near ± 0.1 meV, an $\sim 4\pi$ transmission phase change is possible, *conditional* upon the dot exciton being at the frequency regime—which can be tuned, for example, by applying a field-induced Stark shift. In reflection, conditional phase changes of around $\pm\pi/4$ are found to be possible; note that the one-photon results (i.e., the WEA) tend to overestimate this value. Including the coupling to the phonon bath is seen to qualitatively change the phase characteristics, and we stress that there is no effective γ' which could mimic the same phase trends with phonon bath coupling; the large negative phase of transmission actually widens with increasing γ' , instead of narrowing and then eventually disappears for increasing drives. The phase gate characteristics can be optimized further by changing the phonon bath temperature and by changing the exciton-cavity detuning.

IV. CONCLUSIONS

We have presented a semiconductor ME formalism that can accurately simulate coherent input/output coupling of semiconductor cavity-QED systems such as planar photonic crystals and micropillar cavities. We investigated the role of quantized multiphoton effects and pointed out the possible failure of the WEA, which is shown to fail even for low input powers and small mean cavity photon numbers (much lower than 0.1). For increasing field strengths, the possible failure of the semiclassical approach is also highlighted. We have

further shown that coupling to an acoustic phonon bath causes considerable qualitative changes to the light propagation characteristics than is modeled by a simple pure dephasing process. Finally, we used this model to simulate a conditional phase gate.

ACKNOWLEDGMENTS

This work was supported by the National Sciences and Engineering Research Council of Canada. We thank H. J. Carmichael for useful discussions and acknowledge use of the quantum optics toolbox.³⁶

*shughes@physics.queensu.ca

- ¹J. I. Cirac, P. Zoller, H. J. Kimble, and H. Mabuchi, *Phys. Rev. Lett.* **78**, 3221 (1997).
- ²K. J. Vahala, *Nature (London)* **424**, 839 (2003).
- ³W. Yao, R.-B. Liu, and L. J. Sham, *Phys. Rev. Lett.* **95**, 030504 (2005).
- ⁴J. L. O'Brian, A. Furusawa, and J. Vučković, *Nat. Photonics* **3**, 687 (2009).
- ⁵D. A. Faraon, B. Zhang, Y. Yamamoto, and J. Vučković, *Opt. Express* **15**, 5550 (2007).
- ⁶P. Yao, V. S. C. Manga Rao, and S. Hughes, *Laser Photonics Rev.* **4**, 499 (2010).
- ⁷S. Ates, S. M. Ulrich, A. Ulhaq, S. Reitzenstein, A. Löffler, S. Höfling, A. Forchel, and P. Michler, *Nat. Photonics* **3**, 724 (2009).
- ⁸C. Kistner, K. Morgener, S. Reitzenstein, C. Schneider, S. Höfling, L. Worschech, A. Forchel, P. Yao, and S. Hughes, *Appl. Phys. Lett.* **96**, 221102 (2010).
- ⁹R. Bose, D. Sridharan, G. S. Solomon, and E. Waks, *Opt. Express* **19**, 5398 (2011).
- ¹⁰S. Hughes and H. Kamada, *Phys. Rev. B* **70**, 195313 (2004).
- ¹¹V. Loo, L. Lanco, A. Lemaitre, I. Sagnes, O. Krebs, P. Voisin, and P. Senellart, *Appl. Phys. Lett.* **97**, 241110 (2010).
- ¹²A. B. Young, R. Oulton, C. Y. Hu, A. C. T. Thijssen, C. Schneider, S. Reitzenstein, M. Kamp, S. Höfling, L. Worschech, A. Forchel, and J. G. Rarity, *Phys. Rev. A* **84**, 011803(R) (2011).
- ¹³D. Englund, A. Faraon, I. Fushman, N. Stoltz, P. Petroff, and J. Vučković, *Nature (London)* **450**, 857 (2007).
- ¹⁴A. Auffèves-Garnier, C. Simon, J.-M. Gérard, and J.-P. Poizat, *Phys. Rev. A* **75**, 053823 (2007).
- ¹⁵L. Besombes, K. Kheng, L. Marsal, and H. Mariette, *Phys. Rev. B* **63**, 155307 (2001).
- ¹⁶F. Milde, A. Knorr, and S. Hughes, *Phys. Rev. B* **78**, 035330 (2008).
- ¹⁷U. Hohenester, *Phys. Rev. B* **81**, 155303 (2010); U. Hohenester, A. Laucht, M. Kaniber, N. Hauke, A. Neumann, A. Mohtashami, M. Selinger, M. Bichler, and J. J. Finley, *ibid.* **81**, 201311 (2009).
- ¹⁸S. Hughes, P. Yao, F. Milde, A. Knorr, D. Dalacu, K. Mnaymneh, V. Sazonova, P. J. Poole, G. C. Aers, J. Lapointe, R. Cheriton, and R. L. Williams, *Phys. Rev. B* **83**, 165313 (2011).
- ¹⁹M. Calic, P. Gallo, M. Felici, K. A. Atlasov, B. Dwir, A. Rudra, G. Biasiol, L. Sorba, G. Tarel, V. Savona, and E. Kapon, *Phys. Rev. Lett.* **106**, 227402 (2011).
- ²⁰C. Roy and S. Hughes, *Phys. Rev. Lett.* **106**, 247403 (2011).
- ²¹S. Hughes and H. J. Carmichael, *Phys. Rev. Lett.* **107**, 193601 (2011).
- ²²C. Roy and S. Hughes, *Phys. Rev. X* **1**, 021009 (2011).
- ²³We have also added in vertical cavity decay (Γ_0) to the results in Ref. 10, caused by coupling to radiation modes above the photonic crystal slab (light line).
- ²⁴E. Waks and J. Vučković, *Phys. Rev. Lett.* **96**, 153601 (2006).
- ²⁵J. T. Shen and S. Fan, *Phys. Rev. A* **79**, 023837 (2009).
- ²⁶M. T. Rakher, N. G. Stoltz, L. A. Coldren, P. M. Petroff, and D. Bouwmeester, *Phys. Rev. Lett.* **102**, 097403 (2009).
- ²⁷See, e.g., H. J. Carmichael, *Statistical Methods in Quantum Optics 2* (Springer-Verlag, Berlin, 2008).
- ²⁸G. D. Mahan, *Many-Particle Physics* (Plenum, New York, 1990).
- ²⁹B. Krummheuer, V. M. Axt, and T. Kuhn, *Phys. Rev. B* **65**, 195313 (2002).
- ³⁰I. Wilson-Rae and A. Imamoglu, *Phys. Rev. B* **65**, 235311 (2002).
- ³¹D. P. S. McCutcheon and A. Nazir, *New J. Phys.* **12**, 113042 (2010).
- ³²Y. Ota, S. Iwamoto, N. Kumagai, and Y. Arakawa, e-print arXiv:0908.0788 (unpublished).
- ³³A. Majumdar, E. D. Kim, Y. Gong, M. Bajcsy, and J. Vučković, *Phys. Rev. B* **84**, 085309 (2011).
- ³⁴A. J. Ramsay, A. M. Fox, M. S. Skolnick, A. V. Gopal, E. M. Gauger, B. W. Lovett, and A. Nazir, *Phys. Rev. Lett.* **104**, 017402 (2010).
- ³⁵S. M. Ulrich, S. Ates, S. Reitzenstein, A. Löffler, A. Forchel, and P. Michler, *Phys. Rev. Lett.* **106**, 247402 (2011).
- ³⁶S. M. Tan, *J. Opt. B* **1**, 424 (1999).